



Brief paper

A Gauss–Newton-based decomposition algorithm for Nonlinear Mixed-Integer Optimal Control Problems[☆]

Adrian Bürger^{a,b}, Clemens Zeile^c, Angelika Altmann-Dieses^a, Sebastian Sager^c,
Moritz Diehl^{b,d,*}

^a Institute of Refrigeration, Air-Conditioning, and Environmental Engineering (IKKU), Karlsruhe University of Applied Sciences, Moltkestraße 30, 76133 Karlsruhe, Germany

^b Systems Control and Optimization Laboratory, Department of Microsystems Engineering (IMTEK), University of Freiburg, Georges-Koehler-Allee 102, 79110 Freiburg im Breisgau, Germany

^c Institute for Mathematical Optimization, Faculty of Mathematics, Otto von Guericke University Magdeburg, Universitätsplatz 2, 39106 Magdeburg, Germany

^d Department of Mathematics, University of Freiburg, Ernst-Zermelo-Straße 1, 79104 Freiburg im Breisgau, Germany

ARTICLE INFO

Article history:

Received 26 April 2022

Received in revised form 30 September 2022

Accepted 10 January 2023

Available online xxxx

Keywords:

Mixed-integer optimal control

Switched nonlinear systems

Algorithms and software

ABSTRACT

For the fast approximate solution of Mixed-Integer Non-Linear Programs (MINLPs) arising in the context of Mixed-Integer Optimal Control Problems (MIOCPs) a decomposition algorithm exists that solves a sequence of three comparatively less hard subproblems to determine an approximate MINLP solution. In this work, we propose a problem formulation for the second algorithm stage that is a convex approximation of the original MINLP and relies on the Gauss–Newton approximation. We analyze the algorithm in terms of approximation properties and establish a first-order consistency result. Then, we investigate the proposed approach considering a numerical case study of Mixed-Integer Optimal Control (MIOC) of a renewable energy system. The investigation shows that the proposed formulation can yield an improved integer solution regarding the objective of the original MINLP compared with the established Combinatorial Integral Approximation (CIA) algorithm.

© 2023 The Authors. Published by Elsevier Ltd. This is an open access article under the CC BY license (<http://creativecommons.org/licenses/by/4.0/>).

1. Introduction

Using MIOCPs in real-time control applications requires the fast solution of MINLPs, cf. Kirches (2011). While general MINLP solvers are usually not suitable for this task (Sager, 2009), approximate fast solutions of such MINLPs can be obtained using a decomposition approach which relies on the solution of a sequence of three comparatively less hard subproblems, cf. Sager (2009) and Sager et al. (2012, 2011). The approach has been implemented successfully in various applications such as the control of renewable energy systems (Bürger et al., 2019) and hybrid electric vehicles (Robuschi et al., 2021).

In the second stage of this algorithm, an integer solution for the discrete inputs of the controlled system is computed based on a corresponding relaxed solution determined in the first stage. This is often realized by solving a so-called CIA problem (Sager et al., 2011), which yields an integer approximation with minimum distance to the determined relaxed solution as measured by a dedicated norm. The formulation of this problem, which is a Mixed-Integer Linear Program (MILP) of a special structure, originally relies only on the relaxed integer solution and possibly additional combinatorial constraints for the integer solution, e. g., maximum permissible number of switches (Sager & Zeile, 2021) or minimum dwell times (Zeile et al., 2021), but does not explicitly consider further information of previous algorithm stages, e. g., the effects of the approximated discrete inputs on the system states. Owing to that, approximations obtained using CIA can sometimes lead to poor control performance, depending on the relaxed solution that is processed and the system's sensitivity to its discrete controls, cf. Bürger (2020).

1.1. Relevant literature

With regard to the CIA decomposition, the inclusion of combinatorial constraints for MIOCPs has been investigated via multi-bang or total variation regularization (Leyffer & Manns, 2021);

[☆] The material in this paper was not presented at any conference. This paper was recommended for publication in revised form by Associate Editor Kok Lay Teo under the direction of Editor Ian R. Petersen.

* Corresponding author at: Systems Control and Optimization Laboratory, Department of Microsystems Engineering (IMTEK), University of Freiburg, Georges-Koehler-Allee 102, 79110 Freiburg im Breisgau, Germany.

E-mail addresses: adrian.buerger@h-ka.de (A. Bürger), clemens.zeile@ovgu.de (C. Zeile), angelika.altmann-dieses@h-ka.de (A. Altmann-Dieses), sager@ovgu.de (S. Sager), moritz.diehl@imtek.uni-freiburg.de (M. Diehl).

Manns, 2021; Sager & Zeile, 2021) and using a penalty alternating direction method (Göttlich et al., 2021). Our approach is different from the latter method in the sense that we do not introduce a penalization term in the original problem. To obtain state constraint feasibility of the rounded solution, a forward simulation of differential states as part of the CIA problem was proposed in Lilienthal et al. (2020). Moreover, the steps in the CIA decomposition can be modified and iterated similarly as in the Feasibility Pump algorithm (Fischetti et al., 2005) for MIOCPs for which the feasibility of solutions is difficult to achieve. Apart from the three-step CIA decomposition, a bilevel approach has been proposed to solve MIOCPs, where the switching sequence and switching times are optimized on the upper and lower level, respectively (Bemporad et al., 2002). The idea of switching time optimization (Axelsson et al., 2008; Gerdt, 2006) is to optimize over the durations of the system modes, which results in a Non-Linear Program (NLP). As part of this approach, switching costs can be included (De Marchi, 2019).

Approaches that approximate MINLPs with MIQPs are computationally advantageous and rely, e.g., on Sequential Quadratic Programming (SQP)-type algorithms (Exler et al., 2012) or quadratic outer approximation (Fletcher & Leyffer, 1994). These approaches are closely related to the one presented in this work.

1.2. Contribution

We present a problem formulation for the second stage of the decomposition algorithm that relies on linearization of the original MINLP. In particular, we derive a convex approximation of the original problem that relies on the Gauss–Newton approximation. The solution of this problem, which is an MIQP, can yield an improved integer solution in terms of the objective and feasibility of the original MINLP as it allows for an explicit consideration of information from the first algorithm stage and how the integer approximation affects the system state. We justify the proposed approach theoretically by establishing a first-order consistency result and demonstrate the possible advantages considering a numerical case study of MIOC of a renewable energy system.

1.3. Outline

The remainder of this work is organized as follows: Section 2 formally introduces the class of MIOCPs considered in this work. Section 3 provides a description of the decomposition algorithm. Section 4 introduces different distance functions for use within the second stage of the decomposition algorithm, and a novel Gauss–Newton (GN)-based distance function. The proposed convex approximation is described in Section 5 and its properties are discussed in Section 6. Section 7 states the potential advantages of the proposed approach considering a numerical case study. Section 8 concludes this work.

2. Mixed-integer optimal control problems

This section introduces the MIOCP and the derived MINLP formulation considered in this work. For this, we follow the notation and presentation of Rawlings et al. (2020). The concatenation of a number of vectors $a \in \mathbb{R}^{n_a}$ as in $\mathbf{a} := [a(1)^\top, \dots, a(k)^\top]^\top \in \mathbb{R}^{k \cdot n_a}$ is in the following denoted by the expression $\mathbf{a} := (a(1), \dots, a(k))$.

2.1. Problem formulation

The algorithms and approaches presented in this work are based on a careful formulation of the MIOCP into an MINLP with a special structure. The MINLP is similar to a standard Optimal Control Problem (OCP) in discrete time; however, the inputs comprise continuous inputs u and integer inputs i , such that the system is described by

$$x^+ = f(x, u, i). \quad (1)$$

Without loss of generality, we restrict ourselves to integers $i \in \mathbb{Z}^{n_i}$ inside a bounded convex polyhedron $P \subset \mathbb{R}^{n_i}$. The polyhedral constraint $i \in P$ allows us to exclude some combinations, e.g., if two machines cannot be operated simultaneously. The polyhedron P can and should be chosen as the convex hull of the admissible integer values in each time step. Also, note that an integer program in which all integer variables are constrained so that the possible choices for each integer variable define a finite set, can also be formulated as a binary program using partial outer convexification, cf. Kirches (2011).

We might have additional combinatorial constraints that couple different time steps with each other. We express these coupling constraints in the form of another polyhedron \mathbf{P}_{cpl} in the space of integer control trajectories, which are denoted by

$$\mathbf{i} := (i(0), i(1), \dots, i(N-1)) \in \mathbb{R}^{N \cdot n_i}, \quad (2)$$

where N denotes the number of discretization intervals. The overall polyhedron describing all combinatorial constraints imposed on the integer control trajectory is denoted by

$$\mathbf{P} = P^N \cap \mathbf{P}_{\text{cpl}}. \quad (3)$$

Note that the set of integer feasible trajectories is bounded and given by

$$\mathbf{P} \cap \mathbb{Z}^{N \cdot n_i}, \quad (4)$$

i.e., the intersection of \mathbf{P} with the integers. For notational convenience, we also introduce the sequences of predicted states \mathbf{x} and continuous control inputs \mathbf{u} as

$$\mathbf{x} := (x(0), x(1), \dots, x(N)) \in \mathbb{R}^{(N+1) \cdot n_x}, \quad (5)$$

$$\mathbf{u} := (u(0), u(1), \dots, u(N-1)) \in \mathbb{R}^{N \cdot n_u}. \quad (6)$$

Additionally, we introduce a sequence of vectors of slack variables

$$\mathbf{s} := (s(0), s(1), \dots, s(N)) \in \mathbb{R}^{(N+1) \cdot n_s}, \quad (7)$$

which can be utilized to preserve feasibility of an optimization problem in the case of small constraint violations, which can be relevant for practical applications, cf. Rawlings et al. (2020). Further, we assume that the objective terms consist of a nonlinear least squares term $\frac{1}{2} \|F_1(\cdot)\|_2^2$ and a nonlinear term $F_2(\cdot)$, i.e., they can be written as

$$\ell(x, u, i, s) = \frac{1}{2} \|F_{\ell,1}(x, u, i, s)\|_2^2 + F_{\ell,2}(x, u, i, s), \quad (8)$$

$$V_f(x, s) = \frac{1}{2} \|F_{f,1}(x, s)\|_2^2 + F_{f,2}(x, s). \quad (9)$$

The inequality constraints h and h_f are assumed to be generally nonlinear. Then, the MINLP under investigation can be formulated as

$$\min_{\mathbf{x}, \mathbf{u}, \mathbf{i}, \mathbf{s}} \sum_{k=0}^{N-1} \ell(x(k), u(k), i(k), s(k)) + V_f(x(N), s(N)) \quad (10a)$$

$$\text{s. t. } x(0) = x_0, \quad (10b)$$

$$x(k+1) = f(x(k), u(k), i(k)), \quad (10c)$$

$$k = 0, \dots, N-1,$$

$$h(x(k), u(k), i(k), s(k)) \leq 0, \quad (10d)$$

$$k = 0, \dots, N-1,$$

$$h_f(x(N), s(N)) \leq 0, \quad (10e)$$

$$\mathbf{i} \in \mathbf{P}, \quad (10f)$$

$$\mathbf{i} \in \mathbb{Z}^{N \cdot n_i}. \quad (10g)$$

In the following, we assume that the problem has a feasible solution for any fixed control trajectory $\mathbf{i} \in \mathbf{P}$, considering slack variables for inequality constraint relaxation if necessary. Without the last constraint (10g), problem (10) would be a standard NLP with optimal control structure complicated only by additional couplings between the control variables i that enter via the coupling constraints expressed within the polyhedron \mathbf{P} .

2.2. Notational simplifications

To simplify the notation, we collect all continuous variables in the vector $z = (\mathbf{x}, \mathbf{u}, \mathbf{s}) \in \mathbb{R}^{n_z}$ with $n_z = (N+1)n_x + Nn_u + (N+1)n_s$ and the integer variables in the vector $y = \mathbf{i} \in \mathbb{R}^{n_y}$ with $n_y = Nn_i$. In these summarized variable vectors, problem (10) can be compactly written as:

$$\min_{y,z} F(y, z) = \frac{1}{2} \|F_1(y, z)\|_2^2 + F_2(y, z) \quad (11a)$$

$$\text{s. t. } G(y, z) = 0 \quad (11b)$$

$$H(y, z) \leq 0 \quad (11c)$$

$$y \in \mathbf{P} \quad (11d)$$

$$y \in \mathbb{Z}^{n_y}. \quad (11e)$$

The objective includes the differentiable nonlinear least squares term $\frac{1}{2} \|F_1(\cdot)\|_2^2$ and the differentiable nonlinear term F_2 . The functions G and H contain differentiable nonlinear equality and inequality constraints, respectively. Although the polyhedron \mathbf{P} is convex, the overall problem (11) is nonconvex owing to the integer variables and the generally nonlinear objective and constraint functions.

3. Three-step decomposition algorithm

We assume that there exists a globally optimal solution of MINLP (11) which we denote by (y°, z°) . In most practical applications, the main difficulty is to determine the optimal integer choice y° . If y° would be known, one could just solve an NLP in the remaining variables z to determine the corresponding value z° . This statement can be cleanly expressed if we define the optimal objective function for a fixed $y \in \mathbf{P}$, which we might call the *fixed integer value function*, as follows: $J_{\text{NLP}} : \mathbf{P} \rightarrow \mathbb{R}, y \mapsto J_{\text{NLP}}(y)$ with

$$J_{\text{NLP}}(y) := \min_{z \in \mathbb{R}^{n_z}} F(y, z) \quad (12a)$$

$$\text{s. t. } G(y, z) = 0, \quad (12b)$$

$$H(y, z) \leq 0. \quad (12c)$$

The integer part y° of the MINLP solution is the optimal combinatorially feasible value of this function J_{NLP} , i.e.,

$$y^\circ = \arg \min_y J_{\text{NLP}}(y) \text{ s.t. } y \in \mathbf{P} \cap \mathbb{Z}^{n_y}. \quad (13)$$

Note that a lower bound of the optimal MINLP solution can be obtained by the continuous relaxation

$$J_{\text{NLP}}(y^*) = \min_y J_{\text{NLP}}(y) \text{ s.t. } y \in \mathbf{P}. \quad (14)$$

The lower bound given by (14) inspires the first step of the three-step decomposition algorithm presented in Sager (2009) and Sager et al. (2012, 2011). In the following, a general description of the three algorithm steps S1, S2, and S3 to determine a good feasible solution of MINLP (10) resp. (11) is provided.

S1: In a first step, a *relaxed* version of problem (11), i.e., the NLP that arises if we omit the integer constraint (11e), is solved. The result is a relaxed optimal solution (y^*, z^*) with $y^* \in \mathbf{P}$ but possibly $y^* \notin \mathbb{Z}^{n_y}$.

S2: Afterward, an integer trajectory $y^{**} \in \mathbf{P} \cap \mathbb{Z}^{n_y}$ is heuristically obtained by minimizing some distance function $d(y, y^*)$, i.e., we set $y^{**} := \arg \min_{y \in \mathbf{P} \cap \mathbb{Z}^{n_y}} d(y, y^*)$.

S3: Finally, the integer controls are fixed to y^{**} and the restricted NLP (12) is solved to obtain a solution z^{***} .

The result of the algorithm is typically a feasible but suboptimal solution (y^{**}, z^{***}) for the original MINLP. Owing to optimality, the optimal objective values after steps S1 and S3 equal $J_{\text{NLP}}(y^*)$ and $J_{\text{NLP}}(y^{**})$, respectively. In addition, the value of step S1 equals the relaxed minimum of J_{NLP} , i.e., $J_{\text{NLP}}(y^*) = \min_{y \in \mathbf{P}} J_{\text{NLP}}(y)$. Thus, by construction, steps S1 and S3 provide a lower and upper bound of the true MINLP minimum, i.e.,

$$F(y^*, z^*) \leq F(y^\circ, z^\circ) \leq F(y^{**}, z^{***}). \quad (15)$$

In terms of the nonlinear function J_{NLP} , the same fact can be equivalently stated as

$$J_{\text{NLP}}(y^*) \leq J_{\text{NLP}}(y^\circ) \leq J_{\text{NLP}}(y^{**}). \quad (16)$$

The choice of the distance function in step S2 affects both solution quality and computational complexity, which are typically conflicting objectives. In the remainder of this work, we will discuss different choices for step S2, while steps S1 and S3 will be identical in different variants of the algorithm.

The integer gap between the optimal objective values of (10) and its canonical relaxation, i.e., without (10g), was shown to vanish asymptotically for some \mathbf{P} with the maximal control discretization grid size for binary inputs entering the dynamics (10c) affinely (Sager et al., 2012). While any problem (10) can be reformulated via partial outer convexification (Sager, 2009), we directly assume affinely entering binary inputs for (10) in the following.

4. Distance functions

The perfect choice of distance measure in step S2 would be the suboptimality of $J_{\text{NLP}}(y)$ with respect to the relaxed solution $J_{\text{NLP}}(y^*)$, which we denote by

$$d_{\text{NLP}}(y, y^*) := J_{\text{NLP}}(y) - J_{\text{NLP}}(y^*). \quad (17)$$

This function is nonnegative for all $y \in \mathbf{P}$ and zero for $y = y^*$. While the minimizer $y_{\text{NLP}}^{**} := \arg \min_{y \in \mathbf{P} \cap \mathbb{Z}^{n_y}} d_{\text{NLP}}(y, y^*)$ would equal the optimal integer solution y° of the original MINLP, however, the minimization of this distance function is computationally as expensive as solving the original MINLP.

4.1. Norm-based distance functions

A usually much cheaper choice is to use a norm as distance measure. For a given norm $\|\cdot\|_{\text{norm}}$, one would set

$$d_{\text{norm}}(y, y^*) := \|y - y^*\|_{\text{norm}}. \quad (18)$$

Particularly useful are Linear Programming (LP) representable norms such as the L^1 and L^∞ norm, because the problem $y_{\text{norm}}^{**} :=$

$\arg \min_{y \in \mathbf{P} \cap \mathbb{Z}^{n_y}} d_{\text{norm}}(y, y^*)$ would be an MILP. A particularly successful and widely used norm from this class is the so-called Combinatorial Integral Approximation (CIA) norm that can be defined as

$$\|y - y^*\|_{\text{CIA}} := \|U(y - y^*)\|_{\infty} \quad (19)$$

for a given y^* , where U is a specially chosen invertible matrix, see Sager et al. (2011) for further details. Each row of this matrix computes an integral over one component of the integer control deviation trajectory from the start to an intermediate time point. The MILP to be solved in step S2 would be given by

$$\min_{\theta \in \mathbb{R}, y \in \mathbb{Z}^{n_y}} \theta \quad (20a)$$

$$\text{s. t. } -\mathbf{1}\theta \leq U(y - y^*) \leq \mathbf{1}\theta, \quad (20b)$$

$$y \in \mathbf{P}, \quad (20c)$$

where $\mathbf{1}$ is a vector of all ones and \mathbf{P} would contain a one-hot encoding constraint with regard to the binary controls (Sager et al., 2011). The specific structure of this problem referred to as the CIA problem can be exploited in tailored solution algorithms, cf. Bürger et al. (2020) and Sager et al. (2011). Several surrogate rounding algorithms and problems have been devised instead of solving the CIA problem, e.g., Sum-Up Rounding (Sager, 2009) and SCARP (Bestehorn et al., 2020), where the latter algorithm can also be used to solve the CIA problem. Note that one could define a function

$$J_{\text{CIA}}(y; y^*) := J_{\text{NLP}}(y^*) + \gamma \|y - y^*\|_{\text{CIA}} \quad (21)$$

with arbitrary $\gamma > 0$, which one could interpret as the CIA-approximation of J_{NLP} .

Norm-based distance functions can be advantageous in terms of computational efficiency as the corresponding optimization problems can be solved comparatively fast. However, integer approximations are usually computed based only on y^* as found in step S1 and possibly additional combinatorial constraints, with limited possibility to consider further information from step S1 or the effects of the integer approximation on the system state.

4.2. Novel Gauss–Newton-based distance function

As an intermediate approach that lies between the aforementioned two in terms of ease of computation and approximation accuracy of J_{NLP} , we propose here to use linearizations of the original MINLP founding at (y^*, z^*) . In summary, we will define a convex approximation of J_{NLP} that we denote by $J_{\text{GN}}(y; y^*, z^*)$ and which relies on the GN approximation, cf. Rawlings et al. (2020). The resulting optimization problem is an MIQP, for which we define a nonnegative distance function (to be minimized in step S2) as follows:

$$d_{\text{GN}}(y, y^*) := J_{\text{GN}}(y; y^*, z^*) - J_{\text{NLP}}(y^*). \quad (22)$$

5. Gauss–Newton integer approximation

To formulate the proposed approximation, we first define the linearization of function G at (\bar{y}, \bar{z}) as

$$G_L(y, z; \bar{y}, \bar{z}) := G(\bar{y}, \bar{z}) + \frac{\partial G}{\partial(y, z)}(\bar{y}, \bar{z}) \cdot \begin{bmatrix} y - \bar{y} \\ z - \bar{z} \end{bmatrix}, \quad (23)$$

i.e., its first-order Taylor series expansion. Similarly, we denote the linearization of F and H around (\bar{y}, \bar{z}) by $F_L(y, z; \bar{y}, \bar{z})$ and $H_L(y, z; \bar{y}, \bar{z})$, respectively. We define the quadratic approximation

of F as

$$F_{\text{QP}}(y, z; \bar{y}, \bar{z}, B) := F_L(y, z; \bar{y}, \bar{z}) + \frac{1}{2} \begin{bmatrix} y - \bar{y} \\ z - \bar{z} \end{bmatrix}^{\top} B \begin{bmatrix} y - \bar{y} \\ z - \bar{z} \end{bmatrix}, \quad (24)$$

where B is a positive semidefinite Hessian approximation. An interesting approximation is the squared Jacobian of F_1 from (11a) we call the Gauss–Newton Hessian approximation B_{GN} , which can yield good approximations for least-squares objectives (Rawlings et al., 2020):

$$B_{\text{GN}}(\bar{y}, \bar{z}) := \frac{\partial F_1}{\partial(y, z)}(\bar{y}, \bar{z}) \left(\frac{\partial F_1}{\partial(y, z)}(\bar{y}, \bar{z}) \right)^{\top}. \quad (25)$$

We define F_{GN} as a special case of F_{QP} , in which we set $B = B_{\text{GN}}$. For a given linearization point (\bar{y}, \bar{z}) and matrix B , we define the following MIQP approximation of the original MINLP problem that is given by

$$\min_{y, z} F_{\text{QP}}(y, z; \bar{y}, \bar{z}, B) \quad (26a)$$

$$\text{s. t. } G_L(y, z; \bar{y}, \bar{z}) = 0 \quad (26b)$$

$$H_L(y, z; \bar{y}, \bar{z}) \leq 0 \quad (26c)$$

$$y \in \mathbf{P} \quad (26d)$$

$$y \in \mathbb{Z}^{n_y}. \quad (26e)$$

This MIQP is solved in step S2 of the decomposition algorithm, with the linearization point chosen to equal the relaxed NLP solution, i.e., with $(\bar{y}, \bar{z}) = (y^*, z^*)$.

The MIQP (26) can be relaxed to a convex Quadratic Program (QP) if we drop the integer constraint (26e). This relaxed QP is an approximation of the relaxed NLP, which comes along with a QP approximation of the function J_{NLP} that we denote by J_{QP} and which is defined by $J_{\text{QP}} : \mathbf{P} \times \mathbb{R}^{n_y} \times \mathbb{R}^{n_z} \times \mathbb{R}^{(n_y+n_z) \times (n_y+n_z)} \rightarrow \mathbb{R}, y \mapsto J_{\text{QP}}(y; \bar{y}, \bar{z}, B)$ with

$$J_{\text{QP}}(y; \bar{y}, \bar{z}, B) := \min_{z \in \mathbb{R}^{n_z}} F_{\text{QP}}(y, z; \bar{y}, \bar{z}, B) \quad (27a)$$

$$\text{s. t. } G_L(y, z; \bar{y}, \bar{z}) = 0 \quad (27b)$$

$$H_L(y, z; \bar{y}, \bar{z}) \leq 0. \quad (27c)$$

Given the convexity of the relaxed problem (26) in its variables (y, z) , the function J_{QP} is convex in y . In fact, being the optimal value function of a parametric QP, it is a continuous and piecewise quadratic function, cf. Bank et al. (1983) and Borrelli et al. (2017). As a particular outcome of the QP, we define the Gauss–Newton approximation as

$$J_{\text{GN}}(y; \bar{y}, \bar{z}) := J_{\text{QP}}(y; \bar{y}, \bar{z}, B_{\text{GN}}(\bar{y}, \bar{z})). \quad (28)$$

In step S2, we require $y \in \mathbf{P} \cap \mathbb{Z}^{n_y}$. The idea to use a convex approximation of a possibly nonconvex problem stems from the fact that we linearize around its relaxed optimal solution and a sufficiently close neighborhood of this minimum should be convex.

6. Finite-dimensional approximation properties

In this section, we illustrate the approximation properties of the proposed approach. For this, we first review in Section 6.1 classical results of parametric optimization of Chapter 5.2 in Bonnans and Shapiro (2013), which do not consider integrality constraints.

6.1. Results from parametric optimization

We reconsider the parametric NLP (12) at y , with y being the parameter vector. We consider the linearization of the parametric problem at the optimal solution (y^*, z^*) in the direction $y - y^*$ and define this problem as (LP):

$$J_{LP}(y; y^*, z^*) := \min_{z \in \mathbb{R}^{nz}} F_L(y, z; y^*, z^*) \quad (29a)$$

$$\text{s. t. } G_L(y, z; y^*, z^*) = 0 \quad (29b)$$

$$S_{A(y^*, z^*)} H_L(y, z; y^*, z^*) \leq 0, \quad (29c)$$

where $A(y^*, z^*)$ is the set of active inequality constraints at (y^*, z^*) and $S_{A(y^*, z^*)}$ selects the active inequality constraints of H_L with entries equal to 1 for active constraints and 0 otherwise. The theory in [Bonnans and Shapiro \(2013\)](#) is based on a related LP which we denote as (PL). We define (PL) as (LP) but with $F_L(y, z; y^*, z^*) - F(y^*, z^*)$ as the objective function. Hence, for the corresponding value function holds:

$$J_{PL}(y - y^*; y^*, z^*) := J_{LP}(y; y^*, z^*) - F(y^*, z^*). \quad (30)$$

Let $L(y, \lambda, z)$ be the Lagrangian function associated with NLP (12) at y and we use $\mathcal{S}(\text{DL})$ to denote the set of optimal solutions of the dual of the linearized problem (PL). Finally, we need a strong form of a second-order sufficient optimality condition in the direction $y - y^*$, which states that for all $z - z^* \in C(z^*) \setminus \{0\}$ holds

$$\sup_{\lambda \in \mathcal{S}(\text{DL})} \frac{\partial^2 L}{\partial^2 z}(y^*, \lambda, z^*)(z - z^*, z - z^*) > 0, \quad (31)$$

where $C(z^*)$ is the critical cone associated with z^* . With these definitions, we can state the key result from [Bonnans and Shapiro \(2013\)](#), that we need for this paper.

Theorem 1 ([Bonnans and Shapiro \(2013\)](#)). *Let $\|\cdot\|$ denote a vector norm. Suppose that*

- (1) the unperturbed NLP with $y = y^*$ has a unique optimal solution z^* ,
- (2) the Mangasarian–Fromovitz constraint qualification holds at the point z^* ,
- (3) the set of feasible Lagrange multipliers $\Lambda(y^*, z^*)$ is nonempty,
- (4) second-order sufficient condition (31) is satisfied,
- (5) for all $\|y - y^*\|$ sufficiently small, the feasible set of NLP (12) at y is nonempty and uniformly bounded.

Then, for any optimal solution z of NLP (12) at y holds:

$$\|z - z^*\| = O(\|y - y^*\|), \quad (32)$$

$$J_{NLP}(y) = J_{LP}(y; y^*, z^*) + O(\|y - y^*\|^2). \quad (33)$$

Proof. The results follow from Theorem 5.53, (a) and (b), in [Bonnans and Shapiro \(2013\)](#). In comparison with [Bonnans and Shapiro \(2013\)](#), we replaced Gollan’s condition with the Mangasarian–Fromovitz condition, which is a stronger condition based on Theorem 5.50, (v), in [Bonnans and Shapiro \(2013\)](#). Moreover, we dropped parameterization with $t \geq 0$ of $y(t)$ and $z(t)$ by considering the directions $y - y^*$ and $z - z^*$ in the optimal solution y^* and z^* . Finally, we express (33) with J_{LP} instead of J_{PL} , which are equivalent up to the term $F(y^*, z^*)$. Note that we define (PL) here with the constant constraint terms $G(y^*, z^*)$ and $H(y^*, z^*)$ in contrast to [Bonnans and Shapiro \(2013\)](#). As these terms are zero in the optimum (y^*, z^*) , the constraints of (PL) reduce to the first derivative parts and, thus, are equivalent to the constraints of the linear problem described in [Bonnans and Shapiro \(2013\)](#). \square

6.2. Implications for the proposed algorithm

The following corollary applies the results of [Theorem 1](#) to the QP (27) and the NLP (12).

Corollary 1. *Let the assumptions of [Theorem 1](#) hold for the parametric NLP (12) at $y = y^*$ and assume that the parametric QP (27) at $y = \bar{y} = y^*$ has a unique solution and satisfies the second order condition (31). Then, it holds that*

$$J_{QP}(y; y^*, z^*, B) = J_{LP}(y; y^*, z^*) + O(\|y - y^*\|^2). \quad (34)$$

Furthermore, there is a $C_1 > 0$ and a small $\epsilon_1 > 0$ so that for all $y \in \mathbf{P}_{\epsilon_1} := \{y : \|y - y^*\| < \epsilon_1\}$ holds

$$|J_{NLP}(y) - J_{QP}(y; y^*, z^*, B)| \leq C_1 \|y - y^*\|^2. \quad (35)$$

Proof. While [Theorem 1](#) was so far formulated for the original NLP (12), denoted by $NLP(y)$, at the point $y = y^*$, we can also apply [Theorem 1](#) to the QP (27), denoted by $QP(y; \bar{y}, \bar{z})$, which depends on two sets of parameters, on y and on (\bar{y}, \bar{z}) , but where we assume (\bar{y}, \bar{z}) as fixed to (y^*, z^*) . Thus, $QP(y; y^*, z^*)$ is a parametric problem of the same form as $NLP(y)$ if we only regard its parametric dependence on y . We regard this parametric QP problem again at the point $y = y^*$. To apply [Theorem 1](#) to the $QP(y; y^*, z^*)$, we use the fact that all first order terms of the $NLP(y^*)$ and of the $QP(y^*; y^*, z^*)$ coincide, so assumptions (2), (3), and (5) in [Theorem 1](#) hold because they hold for the original NLP, and by the explicit assumptions also (1) and (4) hold. Also, the corresponding LPs (29) are identical. Thus, (34) follows from the application of [Theorem 1](#) to the $QP(y; y^*, z^*)$ at $y = y^*$.

The inequality (35) follows from the first claim (34) and [Theorem 1](#), (33), by combining these results and expressing the O -notation with the constant C_1 . \square

We remark that the O -notation in the context of integers can be considered as conflicting as the integers y might not be arbitrarily close to y^* . To this end, we introduce the following assumption.

Assumption 1. Consider the set \mathbf{P}_{ϵ_1} from [Corollary 1](#). We assume that for any $\epsilon_1 > 0$, there is a discretization of the MIOCP so that $y^{**}, y^\circ \in \mathbf{P}_{\epsilon_1}$, where y^{**}, y° are the optimal solutions of the MIQP (26) with $\bar{y} = y^*, \bar{z} = z^*$ and the MINLP (11).

This assumption can be deduced as a corollary from [Theorem 3](#) in [Sager et al. \(2012\)](#) if we drop the combinatorial constraints $y \in \mathbf{P}$. However, in the presence of combinatorial constraints it can be restrictive since these constraints can induce a large ϵ_1 and, thus, preventing y from being arbitrarily close to y^* . Based on the above assumption and corollary, the main theoretical result for our algorithm states that the constructed solution y^{**} is correct up to first-order terms with regard to the size of the deviation of the integer controls.

Theorem 2. *Let the assumptions of [Theorem 1](#) hold for the parametric NLP (12), with the optimal solution (y^*, z^*) of the relaxed NLP. Consider the constant C_1 from [Corollary 1](#) for the set \mathbf{P}_{ϵ_1} and let [Assumption 1](#) hold true. Then, we have for the optimal solutions for y^{**} and y° of the MIQP (26) and the MINLP (11)*

$$\begin{aligned} |J_{NLP}(y^{**}) - J_{NLP}(y^\circ)| \\ \leq C_1 (\|y^{**} - y^{**}\|^2 + \|y^* - y^\circ\|^2). \end{aligned} \quad (36)$$

Proof. We abbreviate in the following $J_{QP}(y) := J_{QP}(y; y^*, z^*, B)$. First, note that owing to optimality of y^{**} and y° in MIQP (26) and MINLP (11), resp., it holds that

$$J_{QP}(y^{**}) - J_{QP}(y^\circ) \leq 0. \quad (37)$$

$$J_{NLP}(y^{**}) - J_{NLP}(y^\circ) \geq 0. \quad (38)$$

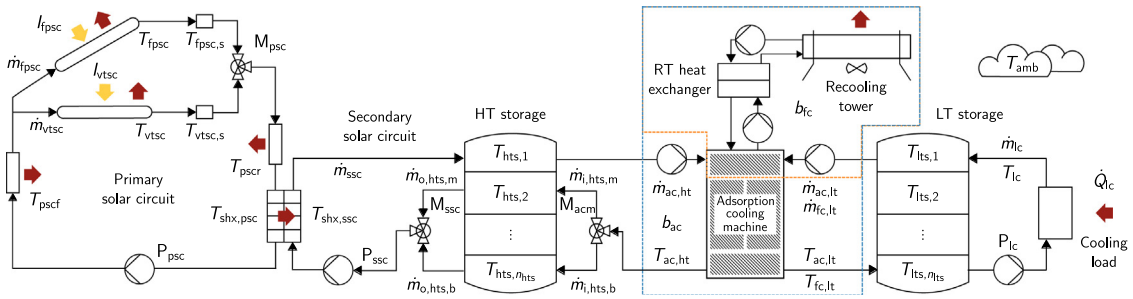


Fig. 1. Schematic of the solar thermal climate system subject to this study.

We use this to derive the result:

$$\begin{aligned}
|J_{\text{NLP}}(y^{**}) - J_{\text{NLP}}(y^\circ)| &\stackrel{(38)}{=} J_{\text{NLP}}(y^{**}) - J_{\text{NLP}}(y^\circ) \\
&= J_{\text{NLP}}(y^{**}) - J_{\text{NLP}}(y^\circ) + J_{\text{QP}}(y^{**}) \\
&\quad - J_{\text{QP}}(y^{**}) + J_{\text{QP}}(y^\circ) - J_{\text{QP}}(y^\circ) \\
&\stackrel{(37)}{\leq} J_{\text{NLP}}(y^{**}) - J_{\text{QP}}(y^{**}) - (J_{\text{NLP}}(y^\circ) - J_{\text{QP}}(y^\circ)) \\
&\leq |J_{\text{NLP}}(y^{**}) - J_{\text{QP}}(y^{**})| + |J_{\text{NLP}}(y^\circ) - J_{\text{QP}}(y^\circ)| \\
&\leq C_1 (\|y^* - y^{**}\|^2 + \|y^* - y^\circ\|^2),
\end{aligned}$$

where we apply in the last inequality [Corollary 1](#) twice for y^{**} and y° . \square

The above result holds for any positive semidefinite matrix B and in particular for the GN-MIQP. Using a suitable vector norm, we may have consistency of order one in the control grid size. By iteratively refining the control grid size, one could possibly establish an asymptotic convergence to the optimal solution, similar to the CIA decomposition ([Jung et al., 2015](#)) but here with quadratic convergence in the grid size. The asymptotic convergence theory can be considered for future studies.

6.3. On the choice of the Hessian approximation

The theoretical results mentioned in the previous section hold regardless of the choice of the Hessian approximation B , as long as it is chosen to be positive semidefinite. However, in practice, the choice is quite relevant. The exact Hessian matrix of the Lagrangian would possibly ensure second-order consistency, however, at the price of expensive computation and possibly indefiniteness. This is in contrast to the pure linearization with $B = 0$, which is inexpensive, but often leads to unfavorably large steps as numerical experiments show. The choice of the GN-approximation appears as a good compromise solution, which is computationally relatively cheap and represents a good approximation of the Hessian matrix.

7. MIOC of a renewable energy system

For this case study we consider a solar thermal climate system located at Karlsruhe University of Applied Sciences, cf. [Bürger et al. \(2021\)](#) for a detailed description. It comprises an Adsorption Cooling Machine (ACM) which can produce cooling energy to cover heat loads of a university building in two different operation modes: in Adsorption Cooling (AC) mode ($b_{ac} = 1$), solar thermal heat can be used to drive the ACM; in Free Cooling (FC) mode ($b_{fc} = 1$), the recoler of the ACM can be used to directly cool down the medium at the ambient in times of low ambient temperature. Heating and cooling energy can be stored in dedicated stratified storages.

An experimental operation of the system using MIOC and CIA was carried out in [Bürger \(2020\)](#) and [Bürger et al. \(2021\)](#). It

showed that insufficient quality of approximated binary controls can lead to less efficient system operation, e. g., through activation of ACM operation modes at unsuitable time periods ([Bürger, 2020](#)). In this case study, the GN-MIQP approach is applied to solve an optimal control problem for the system to achieve efficient system operation in accordance with defined constraints regarding the system's temperature states. The results are compared to those obtained using the CIA approach with regard to solution quality and runtime.

7.1. System modeling and operational constraints

In this study, we use a variant of the existing model and associated constraints presented in [Bürger et al. \(2021\)](#). The model is described by a set of Ordinary Differential Equations (ODEs) as a switched nonlinear system

$$\begin{aligned}
\frac{dx(t)}{dt} &= f_0(x(t), u(t), c(t)) \\
&\quad + \sum_{i=1}^{n_b} b_i(t) \cdot f_i(x(t), u(t), c(t))
\end{aligned} \tag{39}$$

with differential states $x(t) \in \mathbb{R}^{n_x}$, continuous controls $u(t) \in \mathbb{R}^{n_u}$, binary controls $b(t) \in \{0, 1\}^{n_b}$, and time-varying parameters $c(t) \in \mathbb{R}^{n_c}$, with $n_x = 20$, $n_u = 5$, $n_b = 2$, and $n_c = 4$. A schematic is depicted in [Fig. 1](#). For simplicity, the building part of the model in [Bürger et al. \(2021\)](#) is replaced by a simplified load model that facilitates the application of a specific cooling load profile \dot{Q}_c to the system. In particular, the temperature T_{lc} of the medium returning from the fan coil units and corresponding water mass flow \dot{m}_{lc} are calculated as

$$T_{lc}(t) = T_{lts, n_{lts}}(t) + \Delta T_{lc}, \quad \dot{m}_{lc}(t) = \frac{\dot{Q}_{lc}(t)}{c_w \Delta T_{lc}}, \tag{40}$$

with c_w being the medium's specific heat capacity and ΔT_{lc} being an assumed constant temperature difference for the medium returning from the fan coil units.

The system's operational constraints, such as state and control boundaries and minimum dwell times, are summarized in the inequality constraints vector h as

$$h(x(t), u(t), b(\cdot), c(t), s(t)) \leq 0 \tag{41}$$

where we write $b(\cdot)$ to indicate that the constraints for the binary controls can be coupled over time, cf. [Bürger et al. \(2020\)](#). Vector $s \in \mathbb{R}^{n_s}$, $n_s \in \mathbb{N}$ contains slack variables that can be used to relax certain conditions in h , e. g., state constraints, to preserve feasibility if necessary. With regard to the introduction of (40) in the model, the upper and lower limits of the temperature states of the Low-Temperature Storage (LTS) are set to $T_{lts, \max} = 18^\circ\text{C}$ and $T_{lts, \min} = 8^\circ\text{C}$, respectively.

The nonlinear and nonconvex constraints (54) and (55) from [Bürger et al. \(2021\)](#), which are introduced to achieve that the

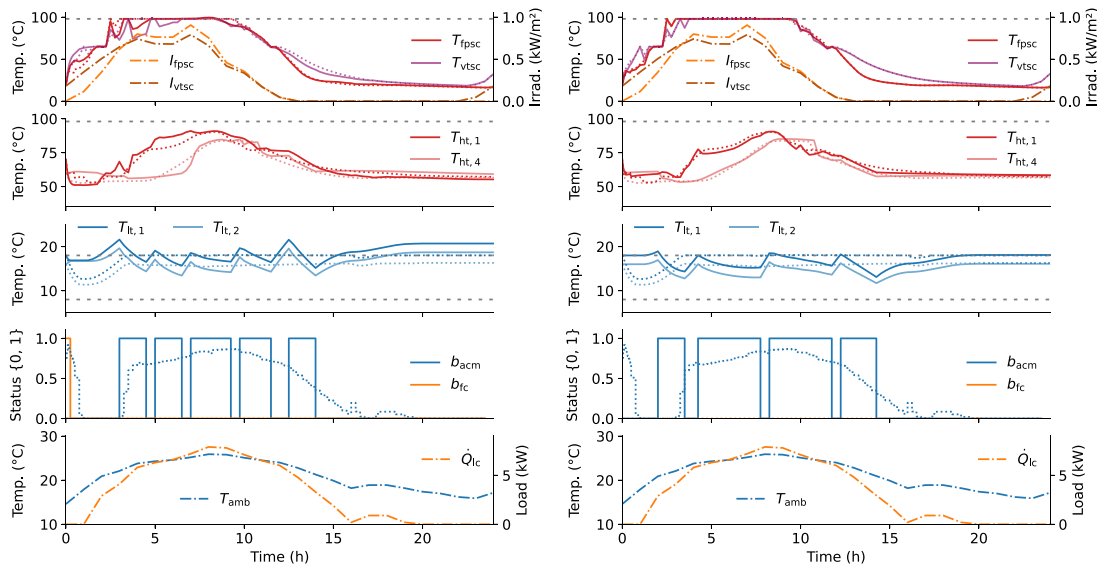


Fig. 2. Results of the CIA (left) and GN-MIQP (right) approaches after step S3 of the decomposition algorithm.

ACM is only operated under suitable conditions with regard to High-Temperature Storage (HTS), LTS, and ambient temperature, are in this work replaced by suitable linear Big-M constraints. While preliminary tests showed that such yielded better solutions in this study both for the CIA and GN-MIQP approach compared to the original formulation, using linear constraints can be advantageous especially for the GN-MIQP approach, since such can even be represented exactly in the GN-MIQP and not only in an approximate form as it is the case for nonlinear constraints.

7.2. Optimal control problem formulation

The aim of the optimal control problem for the system is to compensate the cooling load of the building while keeping the system states, such as storage and collector temperatures, within suitable bounds and reduce the electrical energy consumption of the system. Formulated in continuous time, the used MIOCP reads as

$$\begin{aligned} \min_{\substack{x(\cdot), u(\cdot), \\ b(\cdot), s(\cdot)}} \quad & \frac{1}{2} \int_{t_0}^{t_f} L_1(x(t), u(t), b(t), s(t)) dt \\ & + \int_{t_0}^{t_f} L_2(x(t), u(t), b(t), s(t)) dt \end{aligned} \quad (42a)$$

s. t. for $t \in [t_0, t_f]$:

$$(39),(41) \quad (42b)$$

$$\sum_{i=1}^{n_b} b_i(t) \leq 1, \quad (42c)$$

$$x(t_0) = \hat{x}. \quad (42d)$$

The objective (42a) consists of two Lagrangian terms L_1 and L_2 , where L_1 contains the nonlinear least squares terms and L_2 the linear terms of the objective function. The system model and constraints are included in (42b). Eq. (42c) ensures that at most one ACM operation mode is active at a time and (42d) is the initial state constraint.

7.3. Discretization and implementation

Using a non-equidistant time grid with 91 time steps, cf. Bürger et al. (2021), the MIOCP is formulated as an MINLP using

first discretize, then optimize approaches. For steps S1 and S3, an MINLP is derived using direct collocation (Tsang et al., 1975). For generating the components of the GN-MIQP, an MINLP is derived using direct multiple shooting (Bock & Plitt, 1984) to obtain a matrix G_L that is comparatively smaller than a corresponding matrix derived using direct collocation, with the idea to facilitate a faster solution of the MIQP.

The implementation of the MINLPs is carried out using CasADi (Andersson et al., 2019), the numerical integrator used for the initial guess simulation and within multiple shooting is CVODES (Hindmarsh et al., 2005). The NLPs are solved using Ipopt (Wächter & Biegler, 2006) with linear solver MA57 (HSL, 2019). Combinatorial constraints are neglected in step S1, cf. Bürger et al. (2021). The MIQP is solved using Gurobi (Gurobi Optimization, LLC, 2022) and the CIA problem is solved using the tailored branch-and-bound algorithm in pycombina (Bürger et al., 2020). We provide a sample implementation for a more simple MIOCP application at <https://github.com/adbuenger/gn-miqp-mwe>.

7.4. Numerical results

The CIA and GN-MIQP approaches are used to solve the MIOCP (42) for an exemplary operation scenario. Fig. 2 depicts the results obtained using the CIA approach in the left plots and the solution obtained using the GN-MIQP approach in the right plots. The values of the time-varying parameters c are shown in dash-dotted lines: solar irradiation on the VTSC arrays I_{vtssc} and ambient temperature T_{amb} from an exemplary Test Reference Year (TRY) dataset (Deutscher Wetterdienst (DWD), 2014) depicting a summer day in August, solar irradiation on the oriented FPSC arrays I_{fpssc} calculated using pvlib-python (Holmgren et al., 2018), and a generic cooling load profile \hat{Q}_{ic} . The (identical) solution after step S1 is denoted by dotted lines and the solution after step S3 is denoted by solid lines. The state boundaries considered in the form of soft constraints are indicated using dashed gray lines. It can be observed that the state boundaries of the solar collector temperatures T_{fpssc} and T_{vtssc} as well as the HTS temperatures $T_{hts,\{1..4\}}$ are widely met (only T_{fpssc} and T_{vtssc} limits are slightly violated using the CIA approach). However, this is not the case for the LTS temperatures $T_{lts,1}$ and $T_{lts,2}$.

The LTS temperatures are directly influenced by the binary approximation b_{ac}^{**} and b_{fc}^{**} obtained in step S2 and at the same time widely operated at their upper boundaries in the solution of

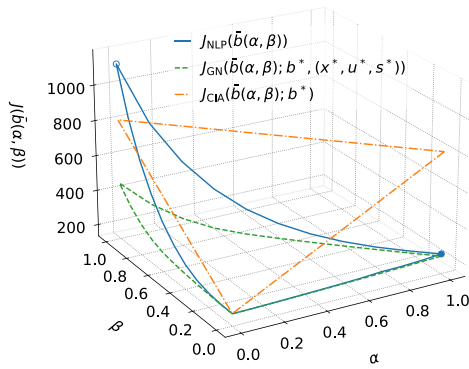


Fig. 3. Evaluation of the functions $J_{\text{NLP}}(\bar{b}(\alpha, \beta))$, $J_{\text{GN}}(\bar{b}(\alpha, \beta); b^*, (x^*, u^*, s^*))$, and $J_{\text{CIA}}(\bar{b}(\alpha, \beta); b^*)$. The value of $J_{\text{NLP}}(b_{\text{GN}}^{**})$ is denoted by \bullet and of $J_{\text{NLP}}(b_{\text{CIA}}^{**})$ by \circ .

step S1. Therefore, an application of the CIA approach which does not consider the development of the system states but only the relaxed binary solution within step S2, can easily violate those temperature boundaries. In contrast, it can be observed that violations of LTS temperature constraints occur less frequently and to a lesser extent while using the GN-MIQP approach. Different from the LTS temperatures, the solar collector temperatures are additionally influenced by continuous controls, e.g., the speed of the pumps P_{psc} and P_{ssc} and the positions of the valves M_{psc} and M_{ssc} , so that their operation can still be adjusted to a certain extent in step S3 according to the binary approximation obtained in step S2. The HTS temperatures are, in addition to the collector operation, influenced by the ACM operation, and with this, by the quality of the obtained binary approximation. However, the HTS is not operated at its upper temperature boundary in this scenario; thus, violations are less likely to occur when an approximated binary solution is applied.

As an additional remark, it can be observed in Fig. 2 that the CIA problem solution contains a short activation of the free cooling mode b_{fc} at the beginning of the control horizon, whereas b_{fc} occurs in the solution of step S1 only to a negligible extent. Similar to the effects described in Bürger (2020), this can be explained by the circumstance that the optimal solution of a CIA problem might not be unique. In the case presented here, the short activation of b_{fc} is not the dominating term of the CIA objective, which minimizes the maximum accumulated difference between the relaxed and binary solution of all binary controls from the beginning of the control horizon up to all time points. While the optimal solution of the CIA problem (20) here yields an objective value of $\theta^* = 1935.6$, the activation of b_{fc} only yields an accumulated difference of 900.0, which is not the maximum accumulated difference. In the solution obtained using the GN-MIQP approach, such activation does not occur.

Fig. 3 shows the values of $J_{\text{NLP}}(\bar{b}(\alpha, \beta))$, $J_{\text{CIA}}(\bar{b}(\alpha, \beta); b^*)$, and $J_{\text{GN}}(\bar{b}(\alpha, \beta); b^*, (x^*, u^*, s^*))$ for (42), with

$$\bar{b}(\alpha, \beta) = b^* + \alpha(b_{\text{GN}}^{**} - b^*) + \beta(b_{\text{CIA}}^{**} - b^*) \quad (43)$$

evaluated for $(\alpha \in [0, 1], \beta = 0)$, $(\alpha = 0, \beta \in [0, 1])$, and $(\alpha + \beta = 1)$. The plot illustrates the piecewise linear approximation yielded by the CIA approach, the piecewise quadratic approximation yielded by the GN-MIQP approach, and that J_{NLP} can be well approximated by J_{GN} locally around the linearization point $b^*, (x^*, u^*, s^*)$.

A runtime comparison for each solution step of both methods is listed in Table 1. The solution times in step S1 are identical since the same problem is solved here. For step S2, the solution of the CIA problem, which was computed using a dedicated solution algorithm (Bürger et al., 2020; Sager et al., 2011), is obtained

Table 1

Runtime of the solution steps for (42).

Step	Runtime CIA (s)	Runtime GN (s)
S1	$2.928 \cdot 10^1$	$2.928 \cdot 10^1$
S2	$9.001 \cdot 10^{-3}$	$2.840 \cdot 10^2$
S3	$1.266 \cdot 10^1$	$1.085 \cdot 10^1$

several orders of magnitude faster compared with the solution of the GN-MIQP (to full optimality). The duration of 284.0s for the GN-MIQP in Table 1 includes the time for setting up the matrix G_L (22.3 s) and solving the problem (261.7 s).

8. Conclusion and future work

We presented a novel MIQP problem formulation for the second stage of an existing decomposition algorithm for fast solution of MIOCPs. First, we established a first-order consistency approximation result for the proposed algorithm. Then, we achieved an improved solution in terms of the original MINLP objective function and overall control performance for a complex application. Since the solution time for the GN-MIQP is rather high compared to the CIA problem, future work could examine its complexity and possibilities to achieve faster GN-MIQP solutions, e.g., if warm-starting based on CIA-based solutions can reduce the runtime and if dedicated solution methods for the GN-MIQP can be developed. Moreover, it could be investigated if suboptimal solutions of the GN-MIQP can already yield an improved control performance, especially in the context of gradually improving an existing CIA result.

Acknowledgments

A. Bürger, A. Altmann-Dieses, and M. Diehl acknowledge funding from INTERREG V Upper Rhine, European Union, Germany, France, project ACA-MODES. S. Sager and C. Zeile acknowledge funding from Deutsche Forschungsgemeinschaft (DFG, German Research Foundation), Germany via GRK 2297 MathCoRe (314838 170) and SPPs 1962 (274039581) and 2331 (441958259). M. Diehl acknowledges funding by DFG, Germany via Research Unit FOR 2401 (277012063) and project 424107692 and by the EU, European Union via ELO-X (953348). We thank four anonymous reviewers whose valuable comments helped to improve and clarify this manuscript.

References

- Andersson, J. A. E., Gillis, J., Horn, G., Rawlings, J. B., & Diehl, M. (2019). CasADi – A software framework for nonlinear optimization and optimal control. *Mathematical Programming Computation*, 11(1), 1–36.
- Axelsson, H., Wardi, Y., Egerstedt, M., & Verriest, E. (2008). Gradient descent approach to optimal mode scheduling in hybrid dynamical systems. *Journal of Optimization Theory and Applications*, 136(2), 167–186.
- Bank, B., Guddat, J., Klatte, D., Kummer, B., & Tammer, K. (1983). *Non-linear parametric optimization*. Birkhäuser Verlag.
- Bemporad, A., Giua, A., & Seatzu, C. (2002). A master-slave algorithm for the optimal control of continuous-time switched affine systems. In *Proceedings of the 41st IEEE conference on decision and control, 2002, Vol. 2* (pp. 1976–1981). IEEE.
- Bestehorn, F., Hansknecht, C., Kirches, C., & Manns, P. (2020). Mixed-integer optimal control problems with switching costs: a shortest path approach. *Mathematical Programming*, 1–32.
- Bock, H. G., & Plitt, K. J. (1984). A multiple shooting algorithm for direct solution of optimal control problems. *IFAC Proceedings Volumes*, 17(2), 1603–1608.
- Bonnans, J. F., & Shapiro, A. (2013). *Perturbation analysis of optimization problems*. Springer Science & Business Media.
- Borrelli, F., Bemporad, A., & Morari, M. (2017). *Predictive control for linear and hybrid systems* (first ed.). Cambridge University Press.
- Bürger, A. (2020). *Nonlinear mixed-integer model predictive control of renewable energy systems* (Ph.D. thesis), University of Freiburg.

- Bürger, A., Bull, D., Sawant, P., Bohlayer, M., Klotz, A., Beschütz, D., Altmann-Dieses, A., Braun, M., & Diehl, M. (2021). Experimental operation of a solar-driven climate system with thermal energy storages using mixed-integer nonlinear model predictive control. *Optimal Control Applications & Methods*, 42(5), 1293–1319.
- Bürger, A., Zeile, C., Altmann-Dieses, A., Sager, S., & Diehl, M. (2019). Design, implementation and simulation of an MPC algorithm for switched nonlinear systems under combinatorial constraints. *Journal of Process Control*, 81, 15–30.
- Bürger, A., Zeile, C., Hahn, M., Altmann-Dieses, A., Sager, S., & Diehl, M. (2020). pycombina: An open-source tool for solving combinatorial approximation problems arising in mixed-integer optimal control. In *IFAC-PapersOnLine*, Vol. 53 (pp. 6502–6508). 21st IFAC World Congress.
- De Marchi, A. (2019). On the mixed-integer linear-quadratic optimal control with switching cost. *IEEE Control Systems Letters*, 3(4), 990–995.
- Deutscher Wetterdienst (DWD) (2014). *Testreferenzjahre von Deutschland für mittlere, extreme und zukünftige Witterungsverhältnisse*. DWD, Offenbach.
- Exler, O., Lehmann, T., & Schittkowski, K. (2012). A comparative study of SQP-type algorithms for nonlinear and nonconvex mixed-integer optimization. *Mathematical Programming Computation*, 4(4), 383–412.
- Fischetti, M., Glover, F., & Lodi, A. (2005). The feasibility pump. *Mathematical Programming*, 104(1), 91–104.
- Fletcher, R., & Leyffer, S. (1994). Solving mixed integer nonlinear programs by outer approximation. *Mathematical Programming*, 66(1), 327–349.
- Gerdt, M. (2006). A variable time transformation method for mixed-integer optimal control problems. *Optimal Control Applications & Methods*, 27(3), 169–182.
- Göttlich, S., Hante, F. M., Potschka, A., & Schewe, L. (2021). Penalty alternating direction methods for mixed-integer optimal control with combinatorial constraints. *Mathematical Programming*, 188, 599–619.
- Gurobi Optimization, LLC (2022). Gurobi optimizer reference manual. <https://www.gurobi.com>, Last accessed September 18, 2022.
- Hindmarsh, A. C., Brown, P. N., Grant, K. E., Lee, S. L., Serban, R., Shumaker, D. E., & Woodward, C. S. (2005). SUNDIALS: Suite of nonlinear and differential/algebraic equation solvers. *ACM Transactions on Mathematical Software*, 31(3), 363–396.
- Holmgren, W. F., Hansen, C. W., & Mikofski, M. A. (2018). pvlb python: a python package for modeling solar energy systems. *Journal of Open Source Software*, 3(29), 884. <http://dx.doi.org/10.5281/zenodo.5366883>, Software version.
- HSL (2019). A collection of Fortran codes for large scale scientific computation. <http://www.hsl.rl.ac.uk/>, Last accessed May 17, 2019.
- Jung, M., Reinelt, G., & Sager, S. (2015). The Lagrangian relaxation for the combinatorial integral approximation problem. *Optimization Methods and Software*, 30(1), 54–80.
- Kirches, C. (2011). *Fast numerical methods for mixed-integer nonlinear model-predictive control*. Vieweg+Teubner Verlag.
- Leyffer, S., & Manns, P. (2021). Sequential linear integer programming for integer optimal control with total variation regularization. Preprint, [arXiv:2106.13453](https://arxiv.org/abs/2106.13453).
- Lilienthal, P., Tetschke, M., Schalk, E., Fischer, T., & Sager, S. (2020). Optimized and personalized phlebotomy schedules for patients suffering from polycythemia vera. *Frontiers in physiology*, 11, 328.
- Manns, P. (2021). Relaxed multibang regularization for the combinatorial integral approximation. *SIAM Journal on Control and Optimization*, 59(4), 2645–2668.
- Rawlings, J. B., Mayne, D. Q., & Diehl, M. M. (2020). *Model predictive control: theory, computation, and design* (second ed.). Nob Hill, 3rd printing.
- Robuschi, N., Zeile, C., Sager, S., & Braghin, F. (2021). Multiphase mixed-integer nonlinear optimal control of hybrid electric vehicles. *Automatica*, 123, Article 109325.
- Sager, S. (2009). Reformulations and algorithms for the optimization of switching decisions in nonlinear optimal control. *Journal of Process Control*, 19(8), 1238–1247.
- Sager, S., Bock, H. G., & Diehl, M. (2012). The integer approximation error in mixed-integer optimal control. *Mathematical Programming (Series A)*, 133, 1–23.
- Sager, S., Jung, M., & Kirches, C. (2011). Combinatorial integral approximation. *Mathematical Methods of Operations Research*, 73(3), 363.
- Sager, S., & Zeile, C. (2021). On mixed-integer optimal control with constrained total variation of the integer control. *Computational Optimization and Applications*, 78(2), 575–623.
- Tsang, T. H., Himmelblau, D. M., & Edgar, T. F. (1975). Optimal control via collocation and non-linear programming. *International Journal of Control*, 21(5), 763–768.

Wächter, A., & Biegler, L. T. (2006). On the implementation of an interior-point filter line-search algorithm for large-scale nonlinear programming. *Mathematical Programming*, 106(1), 25–57.

Zeile, C., Robuschi, N., & Sager, S. (2021). Mixed-integer optimal control under minimum dwell time constraints. *Mathematical Programming*, 188, 653–694.



Adrian Bürger received a M.Sc. degree in Business Administration and Engineering from Karlsruhe University of Applied Sciences in 2014 and a Ph.D. degree from University of Freiburg in 2020. He was a postdoc at Karlsruhe University of Applied Sciences and University of Freiburg, and is currently co-founding the start-up Path to Zero which supports companies in their transition towards a green energy supply. His research interests regard optimization and control applications with a focus on renewable energy systems.



Clemens Zeile studied mathematics at the Universities of Hamburg, Lund, Berkeley and Göttingen, where he also obtained his M.Sc. degree in 2015. He is currently a postdoc at the Otto-von-Guericke Universität Magdeburg, where he also did his Ph.D. in 2021 in the area of mathematical optimization. His research focus lies on the theory and applications of mixed-integer optimal control.



Angelika Altmann-Dieses received her diploma in mathematics in 1997 and her Ph.D. degree in 2000 from Heidelberg University. After working in scientific computing and strategic planning at BASF SE, since 2008 she is a professor for mathematics at the Faculty of Management Science and Engineering and since 2018 the Vice-President for Academic and International Affairs at Karlsruhe University of Applied Sciences. Her research interests regard the optimization and control of energy systems and optimum experimental design.



Sebastian Sager studied mathematics in Heidelberg, where he also obtained his Ph.D. in 2006 and his habilitation in 2012. Since 2012 he is full professor for algorithmic optimization at the Otto-von-Guericke Universität Magdeburg. The focus of his work is on the development of optimization algorithms for problems that combine the properties integrality, nonlinearity, time-dependence, and uncertainty. He uses them in the estimation, control, experimental design, and analysis of dynamic systems and for machine learning. In recent years he has been addressing particular challenges that arise in clinical decision support. He received an ERC Consolidator Grant in 2015 and is spokesperson of the DFG 2297 Research Training Group “Mathematical Complexity Reduction”.



Moritz Diehl graduated with a diploma in physics and mathematics at Heidelberg University and Cambridge University in 1999, and received his Ph.D. degree from Heidelberg University in 2001. From 2006 to 2013, he was a professor with the Department of Electrical Engineering at KU Leuven, Belgium. Since 2013, he is a full professor at the University of Freiburg, Germany, where he heads the Systems Control and Optimization Laboratory at the Department of Microsystems Engineering, and is also affiliated with the Department of Mathematics. His research interests are in optimization and control, spanning from numerical method development to applications in different branches of engineering, with a focus on embedded real-time implementations and renewable energy systems.